Radiophysics and Quantum Electronics, Vol. 47, No. 4, 2004

MULTI-AZIMUTH REGIME OF OBSERVATIONS AT THE RATAN-600 SOUTHERN SECTOR WITH PERISCOPE REFLECTOR

V. M. Bogod,[1]* G. N. Zhekanis,[1] M. G. Mingaliev,[1] and S. Kh. Tokhchukova[2]

UDC 520.24+520.274.3+52-17

This paper is devoted to the development of capabilities of the RATAN-600 radio telescope by putting the regime of multi-azimuth observations at the southern sector with periscope reflector into regular operation. This method makes it possible to study the dynamics of variable radio sources on temporal scales down to a few minutes and increase by one order of magnitude the number of variable sources observed during sky surveys. To date, over ten series of observations of the Sun were performed in the new regime using the multi-wavelength receiver complex, and new astrophysical results were obtained. The software for multi-wavelength mapping of the Sun and wavelet analysis of time series is developed. The following characteristics of the regime are achieved: a temporal resolution of 4 min during a time interval of up to 4.5 h for observations at azimuth angles in the interval from 30° *to* -30°*.*

1. INTRODUCTION

Studies of variable radio source in a wide frequency band and on various typical temporal scales pose problems of frequent observations. In 2000–2003, a regime of multi-azimuth observations was developed and put into regular operation at the southern sector with periscope reflector (SP) of the RATAN-600 radio telescope. The mentioned observations open up new possibilities for studying not only such a variable source as the Sun, but also for performing extensive surveys of variable radio sources. The development of this regime can eventually lead to the development of multi-wavelength observations of pulsars, which is quite important concerning the large effective area of the reflector system. In this paper, this observation regime is used for studying the Sun with the improved temporal resolution. It is known that solar radio astronomers encounter the problem of obtaining images with good spatial, temporal, and spectral resolution in a wide range, and also with high sensitivity with respect to the radiation flux and degree of polarization. Large radio telescopes operable at present (VLA, SSRT, WSRT, OVRO, NoRH, and RATAN-600) make it possible to study the structure of solar formations with spatial resolution to $3{-}15''$. Each of these instruments has specific constraints determining its range of problems. RATAN-600 [1] is a reflector antenna with variable profile of the reflecting surface, large effective area ($400{-}600$ m^2 for one sector), and the operating wavelength range from 50 cm to 8 mm, which is an advantage in comparison with interferometric systems. In combination with panoramic spectrum analyzer (PSA) [2], this radio telescope is the unique instrument for solar research, which provides for simultaneous reception in a wide wavelength range with 5% spectral resolution, high flux sensitivity (a few millijansky), and high accuracy (a fraction of a percent) of measurements of the degree of polarization. At the same time, the relatively low temporal resolution

* vbog@gao.spb.ru

[1] Special Astrophysical Observatory of the Russian Academy of Sciences, Nizhny Arkhyz, Russia; [2] Main (Pulkovo) Astronomical Observatory of the Russian Academy of Sciences, St.Petersburg, Russia. Translated from Izvestiya Vysshikh Uchebnykh Zavedenii, Radiofizika, Vol. 47, No. 4, pp. 255–266, April, 2004. Original article submitted June 6, 2003.

and the fact that the obtained images are one-dimensional are the main drawbacks of RATAN-600 as an instrument for solar studies. Until recently, RATAN-600 was mainly used to obtain one-dimensional images (scans) of radio sources in the transit mode. However, the telescope design permits implementation of a variety of observation regimes including several mapping techniques, such as the azimuth aperture synthesis of two-dimensional images by using the circular reflector and the SP antenna system [1], the near-zenith aperture synthesis [3], or the radio-heliograph regime [4]. In this paper, we consider in more detail the regime of multi-azimuth observations at the SP.

The Sun has been regularly observed at the SP since 1976 in the transit mode. The observations were performed once a day at the local noon (at about 9:13 UT or, with account of the equation of time, from 8:57 to 9:27 UT). In July 1982, the first test series of observations at azimuths ranging from $-8°$ to $8°$ from the meridian was carried out [5]. This made it possible to correct the formulas, obtained earlier by Shivris [6], for calculating the flat-mirror elevation angle and the time of source transit over the antenna beam of the radio telescope with allowance for refraction and variations in the source coordinates during observations. An interactive algorithm was proposed to calculate the antenna setting parameters. This algorithm is used until recently. Based on the observations carried out in July 19, 1982, the first two-dimensional images of an active region on the Sun were obtained at a wavelength of 2 cm [7]. One-dimensional projections of a two-dimensional radio-brightness distribution can be reconstructed both in the signal space and in the Fourier-spectrum space. The second method was chosen at that time because of the limited capabilities of computers (limited RAM resources). In this case, the synthesized position-angle range amounted to $\pm 12°$. The quality of the obtained maps was not high, which impeded their use for astrophysical studies.

Later on, a technique for image synthesis in the signal space was used for azimuthal mapping of the Sun with RATAN-600 [8]. As in the first case, the standard CLEAN procedure (Hogbom algorithm) was used for image correction.

New possibilities for frequent and good-quality multi-azimuth observations at the SP were opened up in the last years owing to automation of the flat reflector [9] and partial automation of the 3rd feed-cabin [10] which was equipped by a high-accuracy "Movitrac 31C" power motor driver manufactured by "Seweurodrive." The driver can be controlled using a computer or the control panel. A solar multi-wavelength receiver complex with unique phase center feed in a broad wavelength range, mounted at the feed cabin, permits simultaneous mapping at 30 wavelengths from 2 to 15 cm.

In addition, increased capabilities of modern computers do not constrain the volume of calculations necessary for mapping with the SP. Improving the image quality and maintaining a user-friendly interface of the software become the main recent problems to be solved in relation to mapping with RATAN-600.

On the other hand, since the amount of information is large (measurements for 61 azimuths at 36 wavelengths yield 2196 scans of the Sun per day), automation of the process of data processing and representation in a form convenient for overview and analysis becomes a topical problem.

In addition to mapping, studies of rapidly varying processes in the solar atmosphere constitute an important line of multi-azimuth observations.

Since 1999, a few series of observations were carried out in the entire azimuth range (from 30° to $-30°$) available to the SP during the months close to the summer/winter solstice (June–July and December) and to the vernal/autumnal equinox (September–October and March–April). The table of observations in put on the Internet and can be found on the web page of the solar study group (SSG) [11].

Observations for a 4-min interval between the successive culminations and a 1-min interval between the successive settings of the antenna system were performed for the first time in March 2002. Such a rate of registration of the solar radio emission is practically ultimate for transit observations of the whole disk (with fixed secondary mirror and cabin) since the Sun passes over the antenna beam (AB) in about 2.5 min while the automatic control system now provides for a circular-reflector setup time of about 1 min.

In principle, to study distinct local sources on the Sun, it is possible to improve the temporal resolution to 2 min between culminations. However, the possibility of full-flux calibration is lost, which makes the requirements for equipment stability during an observation period (up to 4 h) more stringent.

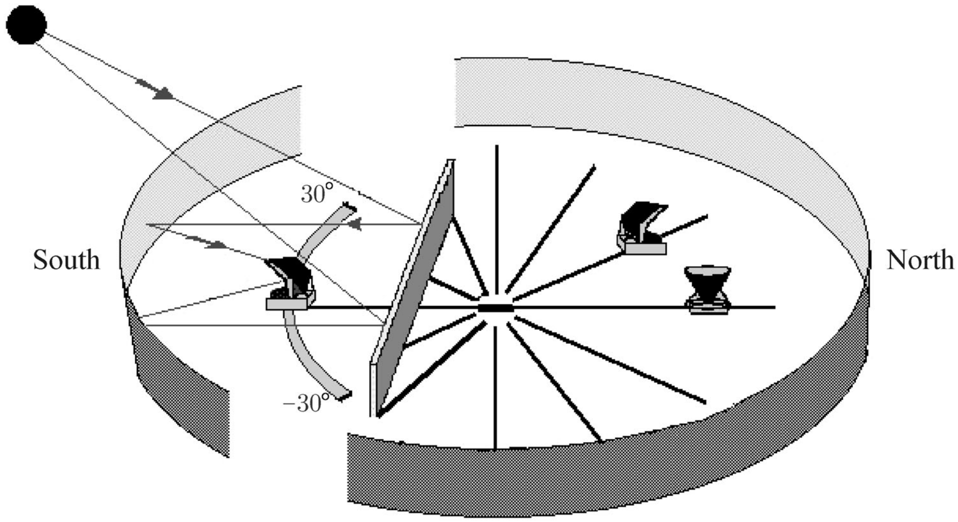

Fig. 1. Scheme of RATAN-600 operation with the use of the antenna system of the southern sector with the flat reflector.

2. METHODICAL FEATURES OF MULTI-AZIMUTH OBSERVATIONS OF THE SUN BY USING THE ANTENNA SYSTEM OF THE SOUTHERN SECTOR WITH PERISCOPE REFLECTOR

The southern sector of the ring reflector of RATAN-600 forms a periscope system together with the flat mirror comprising 124 flat reflecting elements of size $3.1{\times}8.5$ m which can be deflected from the vertical by an angle of up to 70°. The length of the flat mirror is about 400 m. This mirror is oriented exactly in the east–west direction and is located at a distance of 104 m to the south from the radiotelescope center. There is a circular railway track with a curvature radius of 160 m between the flat reflector and the southern sector of the ring reflector. A feed-cabin with the secondary mirror can move along this track, thus providing for observations for azimuths $\pm 30°$ reckoned from the direction to the south (Fig. 1). In contrast to observation regimes without the flat reflector, for which the vertical size of the antenna beam decreases rapidly with increasing position angle of a source, a knife-edge beam is retained at large position angles in the SP system for the above-mentioned azimuth range.

Figure 2 illustrates the features of solar observations with the SP system. These features are related to variation in the orientation of the knife-edge beam with respect to the trajectory of the Sun [6]. It is seen in Fig. 2 that the the orientation of the antenna beam with respect to the axis of the Sun does not vary during time periods close to vernal/autumnal equinox, which is convenient for observations of time-dependent processes. On the other hand, the position angles are maximum during the periods of summer/winter solstice. This is favorable for constructing two-dimensional maps of stable regions on the Sun.

It should be noted that the method of azimuthal mapping is suitable only for studying stable (nonflaring) formations, while multi-azimuth observations with the minimum cadence are necessary for observations of rapidly varying processes, oscillations of the solar atmosphere, and bursts.

Mutual alignment of scans obtained for different azimuths requires allowance for the azimuthal variations in the antenna parameters (the effective antenna area and the AB size). As for the AB size, it should be constant in the first approximation. The effective antenna area is proportional to the product of the cosine of the flat-reflector inclination angle with respect to the vertical and the cosine of the secondary-mirror azimuth [6]. This dependence is plotted in Fig. 3. In the equinox periods when the flat-reflector inclination angle with respect to the vertical is almost constant, the effective antenna area decreases as the cosine of the secondary-mirror azimuth. This decrease amounts to 15% for the azimuths close to $\pm 30°$, while this value becomes 30% for the solstice periods. The mentioned effect holds especially for the long wavelengths. For

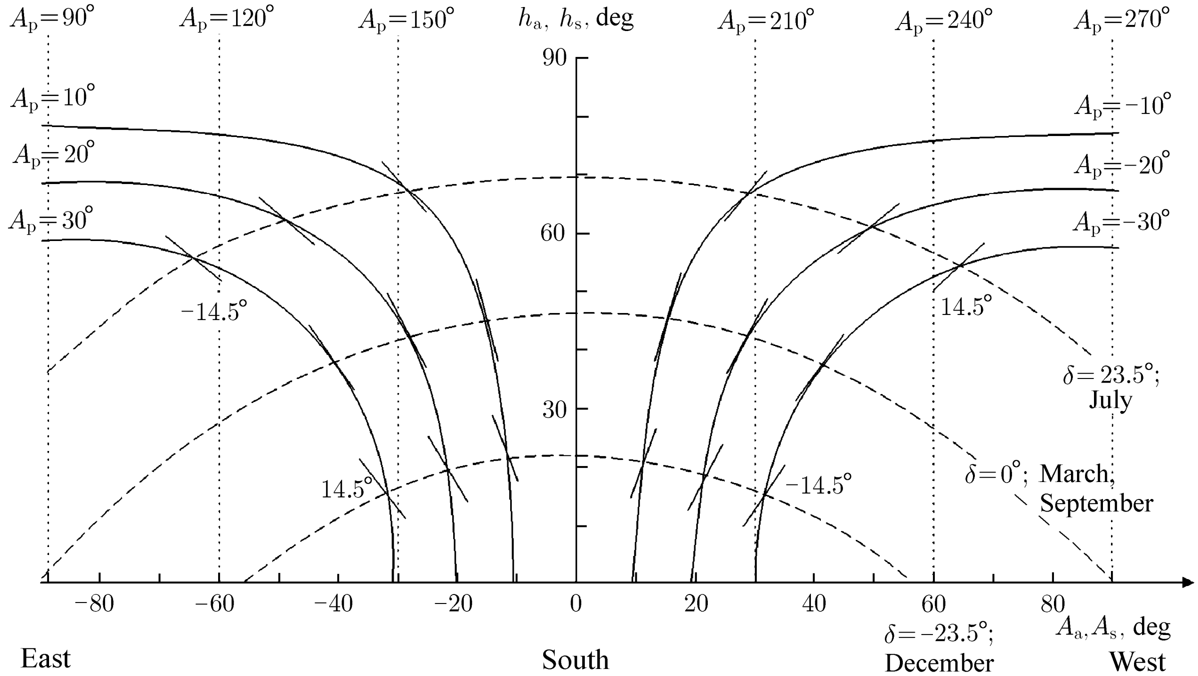

Fig. 2. Trajectories of a source (dashed semicircles) and the AB center (solid curves) for various declinations δ of a source. The orientations of the vertical beam of the antenna are shown by the rectilinear segments at the crossing points of the solid and dashed lines. It is shown that the AB orientation with respect to a source does not change if $\delta = 0°$. If the declination $\delta \approx \pm 23°$, then the position angle ranges from $-14.5°$ to $14.5°$ for observations in the azimuth interval from $-30°$ to $30°$. Here, A_p is the azimuth of the vertex of the parabola along which the elements of the circular reflector of the telescope are set up, A_a and h_a are the azimuth and the inclination angle of the center of the antenna beam, respectively, and A_s and h_s are the azimuth and the position angle of the source, respectively.

the short wavelengths, the cosine of the flat-reflector inclination angle does not affect the decrease in the effective antenna area since the vertical size of the receiving surface is limited by the vertical size of the secondary mirror, which is equal to 5.5 m. For the solar declinations, the secondary-mirror height is *a fortiori* less than the flat-reflector height (7.4 m) multiplied by the cosine of its inclination. As a result, the upper curve in Fig. 3 holds at the short wavelengths irrespectively of the observation period, i.e., both in the solstice and in the equinox. Total-flux calibration makes it possible to perform calibration of the azimuth observations, but actually there are some discrepancies with the calculated parameters (Fig. 3). The maximum discrepancies correspond to the eastest azimuths, from $-30°$ to $-26°$, for which the antenna temperature in the equinox decreases by 30% (instead of the expected 15%) with respect to the meridional value. The discrepancy for other azimuths does not exceed 5%.

Complexity of the considered three-mirror antenna system impedes clarifying the causes of this and other errors. Some errors (e.g., errors of calculation of the culmination time and errors of the reference points for the secondary-mirror setting by azimuth) were revealed during observations and minimized. Other errors, e.g., the vertical shift of the antenna beam, should be taken into account during the data processing. Below we describe the main types of errors affecting the quality of observations, as well as the techniques for determination of these errors from observations of the Sun. All the errors can be classified into two main groups: (i) the errors of the antenna-system positioning by azimuth and (ii) the errors of antenna elevation setting.

The first group includes the circular-reflector setting errors, the flat-reflector setting errors, and the errors of secondary-mirror positioning by azimuth. The circular-reflector setting accuracy is mainly determined by the accurate determination of coordinates of the null points of reflecting elements and the

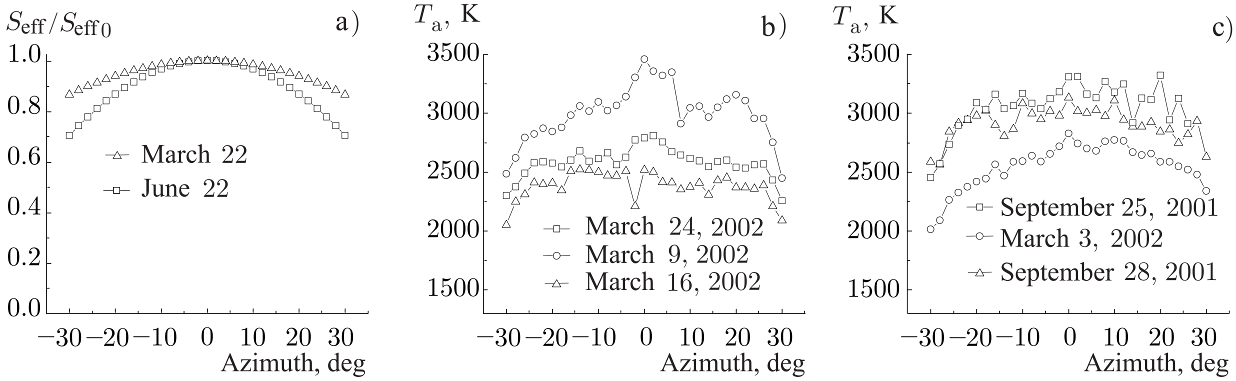

Fig. 3. (*a*) Calculated relative decrease (with respect to the meridional value) in the effective antenna area $S_{\rm eff}$ for observations at various azimuths. The effective area for azimuths close to $\pm 30°$ decreases by up to 15% and 30% in the equinox (March or September) and solstice (December of June) periods, respectively. (*b*) Azimuthal dependence of the antenna temperature $T_{\rm a}$ at a wavelength of 3.21 cm for observations of the quiet Sun using short-aperture settings with 109 circular-reflector elements. (*c*) Azimuthal dependence of the antenna temperature for full-aperture settings with 166 circular-reflector elements.

antenna-surface adjustment accuracy. The effects of these errors are most pronounced at the short wavelengths.

The flat-reflector setting errors have the minimum effect on the quality of observations. An azimuthal turn of the entire flat reflector, which resulted in the appearance of a beam sidelobe, was revealed and reduced to an acceptable value.

The errors of the secondary-mirror positioning at a specified azimuth are seen most clearly in the observation results, so these errors can easily be identified and monitored. At present, secondary-mirror repositioning is controlled by operators using the control panel. Test observations in the automatic-control regime with the use of a computer showed that the distance traveled by the feed-cabin along the railway track corresponds to the expected angular displacement with an accuracy of about 0.01%, which yields an error of up to 1.5 cm for movements from one azimuth to the next. To exclude systematic errors, we composed a map of reference-point label positions on the arched railway track, which has the form of a table of distances between the azimuths in motor rotation increment units. This table is used by the program controlling the driver. This program was developed to implement automatic repositioning of the secondary mirror during multi-azimuth observations. However, the backlash errors impeded achieving the positioning accuracy required for observations at the short wavelengths. Hence, the capabilities of the accurate digital driver are not fully explored at present. A more complicated control system with feedback is necessary for these purposes. Information concerning the computer control of the driver and the reference-point label positions is given on the Internet (see the web page of the solar study group [12]) in "Handbook for observations of the Sun at RATAN-600," see "User's guide for observations using feed No. 3").

Another source of errors is related to temperature variations in the reference-point label positions which can exceed 1 cm. More stable side-mounted reference point labels are now located with only 4° step. Such reference points are planned to be mounted with 2° step. This will improve the accuracy of secondary-mirror positioning. We should also mention the secondary-mirror leveling error. If the interval between azimuthal observations is equal to 1 min, then it is impossible to perform the operator-controlled leveling. In this case, automatic setting of the mirror should be used (such a system is realized for feed No. 1).

Thus, a combination of the errors of secondary-mirror positioning at a specified azimuth, calculation of the culmination time, and azimuthal pointing of the circular and flat reflectors can give rise to aberrations and to a difference between the calculated culmination time and the time when the Sun center is passed during scanning. Figure 4 shows the results of measurements of the total error of azimuthal pointing for a shift of the local-source maximum from the meridian upon correction of the reference-point label positions.

If the error is assumed to be determined by the accuracy of secondary-mirror positioning at a specified

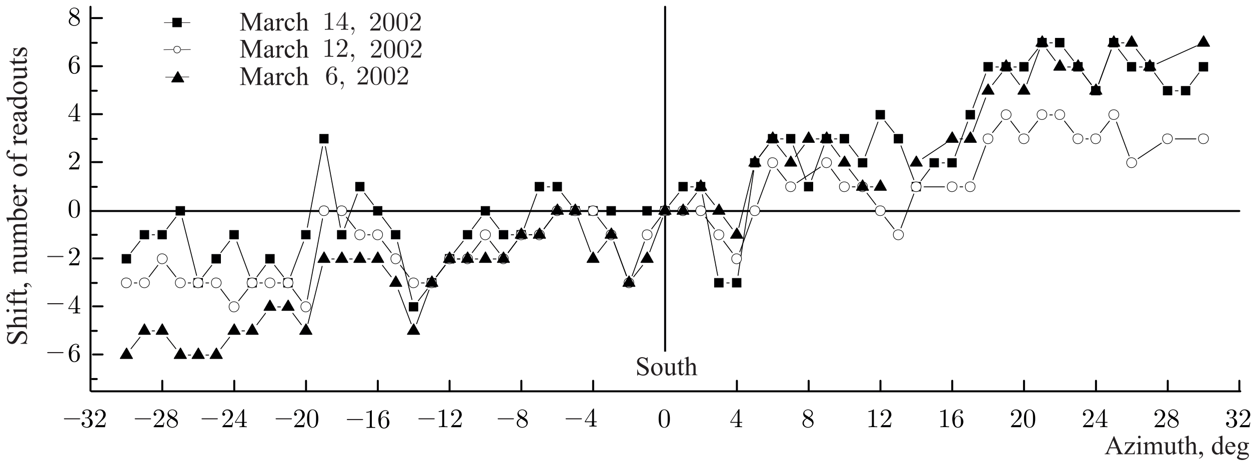

Fig. 4. Plot of the shift of a local-source maximum from the meridian for azimuthal observations. The number of readouts is reckoned on the vertical axis. One readout corresponds to about 5 arcsec on the sky. The slope of the curves is stipulated by the displacement of the source due to rotation of the Sun. Deviations from the inclined straight line are determined by the total effect of the errors of secondary-mirror positioning and the errors of antenna focusing and pointing.

azimuth, then the rms deviation amounts to about 3 mm in terms of the distance along the railway track. Such errors do not lead to noticeable aberrations. A procedure of alignment of the scans is usually used in the “WorkScan” program [13] for reconstruction of the source center. This method yields inaccurate results if there are sources at the solar limb. In this case, alignment with respect to the maximum of the signal from a stable local source on the Sun is used in our software.

As for the errors of antenna elevation setting, their effect on the image quality is weaker since the AB size in the major part of the operating wavelength range is larger than the size of the Sun. Nevertheless, these errors should also be measured and taken into account when calculating radiation fluxes of local sources at the short wavelengths. Using a special technique, we revealed a systematic vertical shift of the antenna beam, which ranges from -4 to -6 arcmin for all wavelengths and azimuths. Such an error can result from, e.g., insufficiently accurate ephemeris calculation (for example, due to inaccurate allowance for refraction) or inaccurate determination of the null points of the reflecting elements. To clarify the causes of the AB shift, it is necessary to observe calibrator sources at various azimuths. To calculate the radiation fluxes of local sources at the short wavelengths (less than 4 cm), it is necessary to take into account that the altitude of the Sun changes during the time of passage of the solar disk over the AB (this time is about 2.5 min), namely, it increases in the morning hours and decreases in the afternoon hours. Variation in the Sun elevation during one observation amounts to about 10 arcmin in the solstice periods. Because of this effect, the AB passes over the Sun not along a straight line, but along some curve in the north-west−south-east and south-west−north-east directions in the morning and afternoon hours, respectively. The position angle $q = -\arcsin(\tan A \tan\delta)$ increases and decreases this slope by up to $h_1 = R_\odot \sin q = 16\sin(14.5°) = 4$ arcmin, where $R_\odot$ is the angular radius of the Sun, in summer and winter, respectively.

For observations with enhanced temporal resolution, the number of reflecting elements was decreased from 166 to 109. This diminished the time of antenna pointing and the effect of beam errors. Measurements of the sizes of a local source on the Sun showed that the AB sizes are retained in a large range of azimuthal angles, and a noticeable broadening of the beam with respect to the meridional value can occur only for the eastest azimuths (from $-26°$ to $-30°$). We recommend not to use these azimuths for mapping purposes until the image quality is improved by adjustment and by using the elements of the adjacent sectors for observations.

3. MULTI-WAVELENGTH MAPPING WITH AZIMUTHAL APERTURE SYNTHESIS

To process the data of multi-azimuth observations, we developed new software in the IDL environment with the use of the standard FITS format and the ASTROLIB libraries. This software package RAIS [14] has a graphical interface, is operable in both the batch and interactive mode, and is open to modification by the user. The software allows one to construct maps of the whole disk of the Sun from the input data obtained in observations both at the SP and in other modes, in particular, for the "zoned relay" method of observations [15]. The mapping technique includes synthesis of a two-dimensional brightness distribution from one-dimensional profiles obtained by scanning an object with beams having knife-edge patterns. The procedure for constructing a synthesized image is based on an algorithm for summation of the corresponding values of one-dimensional profiles [16]:

$$g(x, y) = \sum g_{qi} \, (x \cos q_i + y \sin q_i). \tag{1}$$

The obtained "dirty" map $g(x, y)$ is equivalent to the convolution of the initial image $f(x, y)$ of an object with the synthesized antenna beam h:

$$g(x_0, y_0) = \iint h(x - x_0, y - y_0) f(x, y) \, \mathrm{d}x \, \mathrm{d}y + n(x_0, y_0). \tag{2}$$

Here, $n(x_0, y_0)$ is random noise.

Mathematically, reconstruction of the initial brightness distribution f is a problem of inversion of a linear convolution-type Fredholm equation of the first kind. In the considered case, this problem is solved using the CLEAN algorithm.

Correspondingly, the process of constructing a map consists of the four main procedure commands (Fig. 5):

— synthesis of a "dirty" map (MAP CALC command);

— construction of a "dirty" synthesized beam (2D BEAM CALC);

— calculation of a "clean" two-dimensional beam (2D BEAM CLEAN);

— cleaning of a "dirty" map (MAP CLEAN).

Figure 5*a* shows one-dimensional scans of the whole solar disk, obtained at a wavelength of 2.24 cm in December 19, 2001. The next Fig. 5*b* presents zoomed-in scans of an active region in the eastern hemisphere, obtained for various position angles. It is seen that the source whose signal for the first azimuth consists of one peak and an extended background is eventually, by the last azimuth, resolved into three sources of approximately equal brightness. The obtained "dirty" map is presented in Fig. 5*c*. Since the synthesized beam has sidelobes, the images of the sources also comprise sidelobes, i.e., are "dirty." The algorithm for cleaning sidelobes by the CLEAN procedure includes finding brightness maxima of an image, subtracting the "dirty" beam from these maxima, and adding the "clean" beams (multiplied by a certain gain factor) to them. A "dirty" two-dimensional beam is calculated in the same way as a "dirty" map, but the summation of scans is replaced by summation of the same angle projections of the one-dimensional beam. A "clean" two-dimensional beam is obtained by inscribing a two-dimensional Gaussian distribution into the core of the "dirty" beam (Fig. 5*f*). The size of the synthesized beam at a wavelength of 3.21 cm is $20'' \times 155''$. The vertical size of the "clean" beam is the less the larger the position-angle sector. In the case of the SP, this sector is limited by the geometry of the system since the maximum sector of position angles is about from -14.5° to 14.5° for the railway-track opening angle from 30° to -30°. Thus, instead of a knife-edge beam, we obtain a beam with limited sizes over two coordinates, while the sources are stretched along the vertical. As for the angular resolution between one-dimensional images, it is necessary to have 150 sections with equal angular spacing for the accurate reconstruction of a two-dimensional distribution of the radio brightness of the Sun [17]. Since, in our case, the sector is equal to 30° instead of 180° for the complete coverage of the uv-plane, it suffices for mapping purposes to use 25 and 18 scans in the azimuth ranges

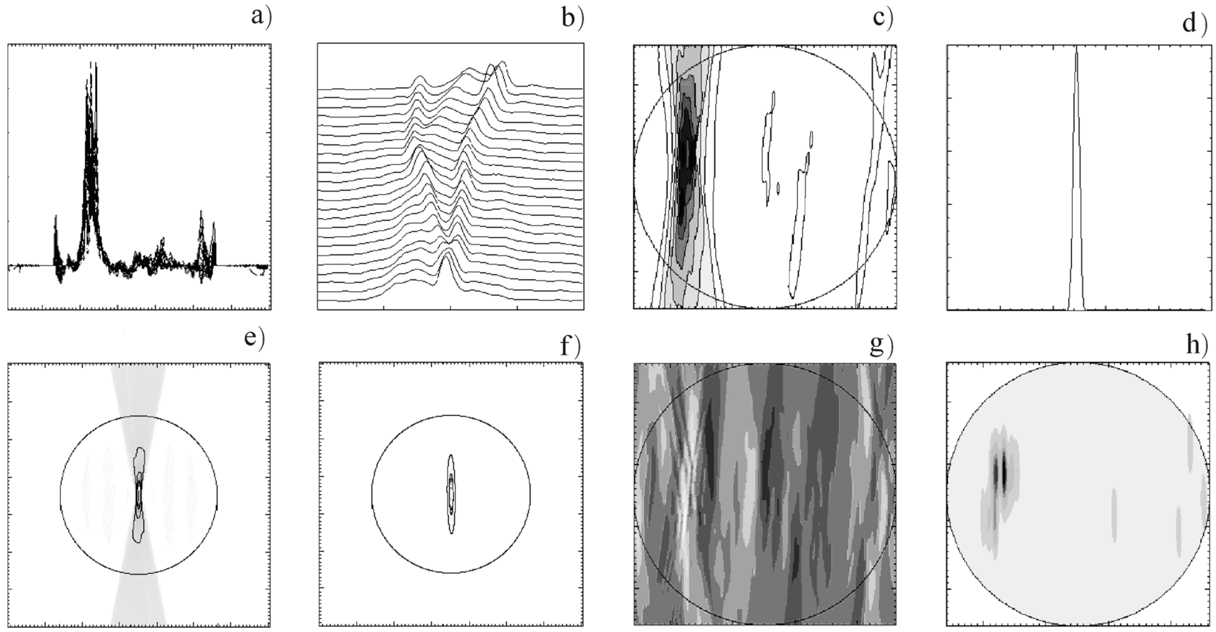

Fig. 5. Visualization of the main stages of mapping. One-dimensional scans of the Sun (*a*); the horizontal size is 20% larger than the optical-disk size. Scans of single active region (*b*); the horizontal size is about 7 arcsec. The "dirty" two-dimensional map (*c*); the circle shows the optical disk of the Sun. One-dimensional beam at a wavelength of 2.24 cm (*d*); the half-width of the beam is about 20 arcsec. The "dirty" synthesized two-dimensional beam (*e*). The "clean" two-dimensional beam (*f*). The residuals after subtraction of the sources from the "dirty" map (*g*); the standard deviation is 1.5% of the maximum of the initial map. The "clean" two-dimensional map of the Sun (*h*).

from 30° to −30° and from 20° to −20°, respectively. Observations with an azimuth step of 2° yield exactly the necessary numbers of images. One also should not forget about another important factor affecting the quality of synthesized two-dimensional images, namely, the accuracy of subtraction of the radiation of the quiet Sun. An example of multi-azimuth mapping of an active region on the Sun at 10 wavelengths in the centimeter wave band is shown in Fig. 6.

4. OBSERVATIONS OF VARIABLE RADIO SOURCES

Analysis of temporal variations in emission from sources on temporal scales from minutes to hours is a research line that is not yet fully explored at RATAN-600.

An example of SP observations for 61 azimuths is presented in Fig. 7. This figure shows the superposition of one-dimensional distributions of the intensity I and the circular polarization V, as well as the dynamics of the antenna-temperature maxima of two local sources on the scan. It is seen that a burst occurred in the leading spot during the observation, while the trailing spot was relatively stable.

To date, various kinds of circular polarization inversion were eventually observed in the emission from solar active regions. Multi-azimuth observations made it possible to observe the dynamics of these phenomena and to point out their relationship to the preflare state of powerful active regions [18]. Further studies in this field and comparison with data for other wavelength ranges can facilitate developing the picture of the onset of a solar flare and help choosing the most realistic flare scenario among a variety of theoretical models.

The method also provides for the unique possibilities for studying magnetic-field oscillations in the chromosphere and corona. The high sensitivity and resolution of the telescope along with the PSA spectral resolution at wavelengths 1−4 cm permits detecting even small magnetic-field variations in the chromosphere, transition region, and corona. Wavelet analysis of multi-azimuth data allowed us to discover oscillations

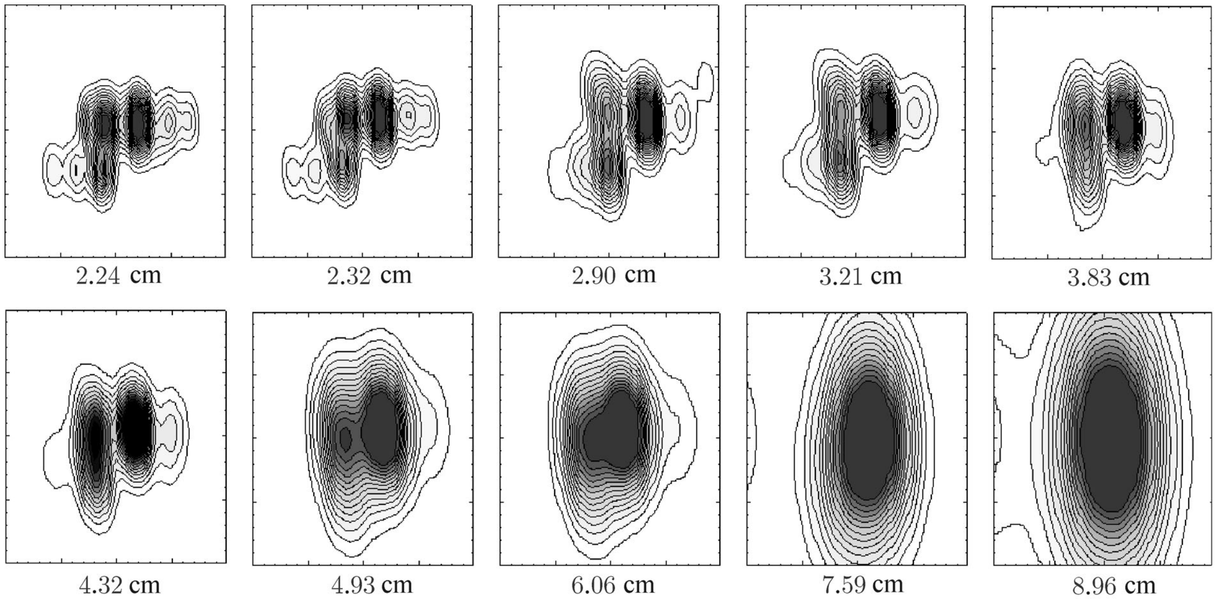

Fig. 6. Synthesized maps of an active region on the Sun at 10 wavelengths from 2.24 to 8.96 cm observed with the SP of RATAN-600. The horizontal and vertical sizes of each image are 4 and 8 arcsec.

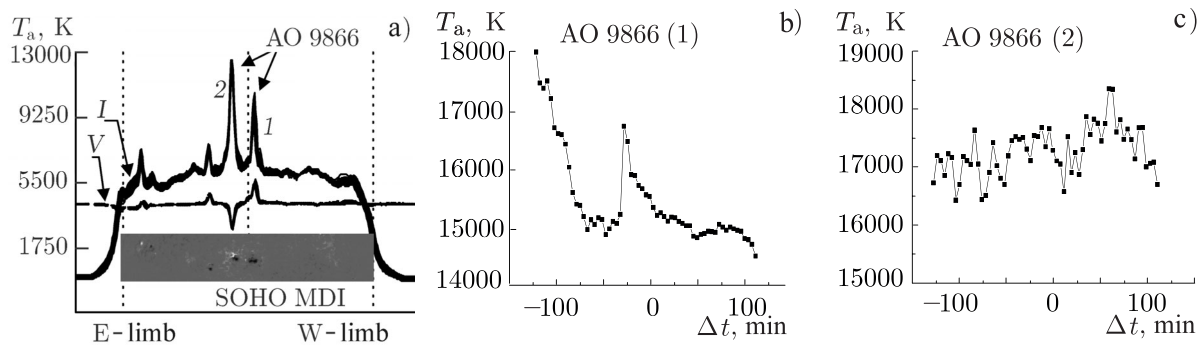

Fig. 7. Superposition of 61 azimuthal scans and comparison with the magnetic fields according to the SOHO MDI data (*a*). The standard deviation of the antenna temperature of a point on the quiet Sun is equal to 1%. Variations in the antenna temperature with the azimuth: the leading (*b*) and trailing (*c*) spots (sources *1* and *2* in the left panel, respectively).

of radio brightness of active regions. Such oscillations have various periods among which the periods of 80 and 50 min are most prominent (Fig. 8). Studying oscillations with a period of about 3 min is also of great interest. The further development of the observation regime and the reduction of the time interval between observations to 2 min will possibly yield new data on the origin of these oscillations.

5. CONCLUSIONS

Implementation of the regime of multi-azimuth observations at the SP makes it possible to carry out the following.

1) A few series of observations of the Sun in the azimuth range from 30° to −30° with temporal resolution reaching 4 min (the interval between the scans is 1 min) during 4–4.5 hours were carried out at RATAN-600 for the first time.

2) To maintain multi-azimuth observations, we modified the existing software and developed new software for processing and analysis of data of multi-azimuth observations, including

— analysis of variations in the emission from various formations on the Sun,

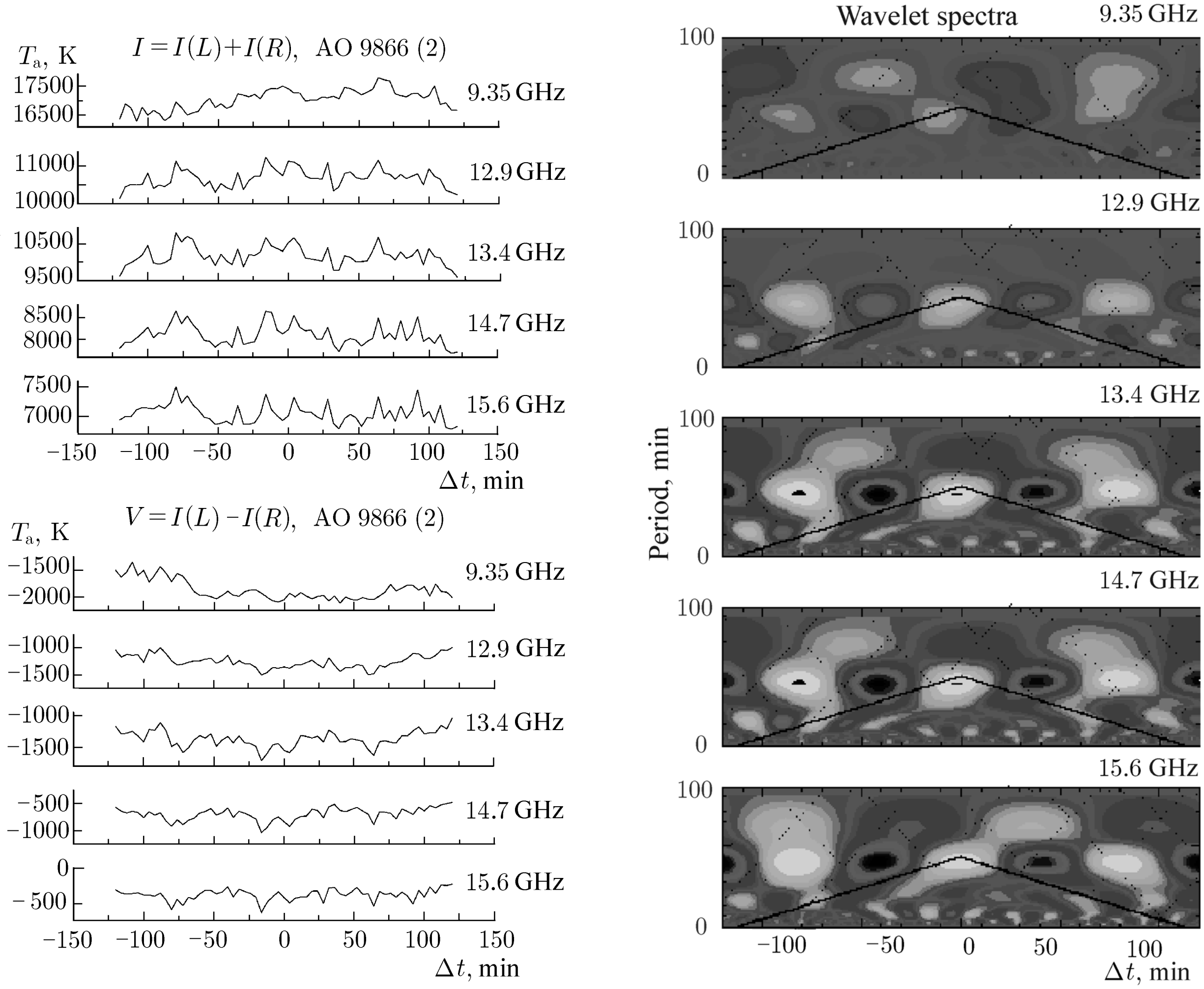

Fig. 8. Time series for the Stokes parameters I and V of a local source in the trailing part of AO 9866 (left) and the wavelet spectra of the same source at a few frequencies in the short-wavelength part of the PSA bandwidth [2] (right). The solid lines in the spectra correspond to cosine of the confidence of periods. In most cases, a period of 80 min is seen in the spectra. However, the duration of realization is not enough for unambiguous conclusion on the reliable detection of these oscillations. A version of the code [19] was used for wavelet analysis of the data.

— multi-wavelength mapping.

A number of astrophysical results were obtained on the basis of observations in the new regime [18, 20]. Implementation of this observation regime also opens up new prospects for other (not solar) branches of studying variable radio sources with RATAN-600.

The authors acknowledge the support by the Russian Foundation for Basic Research (project Nos. 02–02–16430, 03–02–06714, and 02–07–90247) and INTAS (project Nos. 00–0181 and 00–0543), which was important for this work.

REFERENCES

1. Yu. N. Parijskii and O. N. Shivris, *Izv. Glavn. Astron. Obs.*, **188**, 3 (1972).
2. V. M. Bogod, S. M. Vatrushin, V. E. Abramov–Maksimov, S. V. Tsvetkov, and V. N. Dikii, "Panoramic radiometric spectrum analyzer with digital processing of information for the 3.5 − 18 GHz band" [in Russian], preprint No. 84, Special Astrophys. Obs. Russian Acad. Sci., Nizhny Arkhyz (1993).

3. Yu. N. Parijskii, “RATAN-600 and aperture synthesis” [in Russian], preprint No. 33L, Special Astrophys. Obs. USSR Acad. Sci., Nizhny Arkhyz (1986).
4. G. B. Gelfreikh and L. V. Opeikina, “Modeling RATAN-600 operation in the radio-heliograph regime” [in Russian], preprint No. 96, Special Astrophys. Obs. Russian Acad. Sci., Nizhny Arkhyz (1992).
5. V. M. Bogod, B. S. Minchenko, Z. E. Petrov, Yu. K. Zverev, et al., “Results of coordinated observations of the Sun with the RATAN-600 (the southern sector with perisope at 5 azimuths) and VLA (USA) radio teslecopes in July 1982” [in Russian], Special Astrophys. Obs. Report (1983).
6. O. N. Shivris, *Izv. Spets. Astrofiz. Obs.*, **12**, 134 (1980).
7. B. S. Minchenko, *Izv. Spets. Astrofiz. Obs.*, **21**, 91 (1986).
8. A. Nindos, C. E. Alissandrakis, G. B. Gelfreikh, V. N. Borovik, A. N. Korzhavin, and V. M. Bogod, *Solar Phys.*, **165**, 41 (1996).
9. G. V. Zhekanis, in: *Abstracts Conf. “Radio Telescopes RT–2002. Antennas, Equipment, Techniques,” Oct. 9–11, 2002* [in Russian], p. 45.
10. V. B. Khaikin, E. K. Majorova, I. G. Efimov, O. A. Victorov, V. M. Bogod, and S. Kh. Tokhchukova, in: *Proc. VIII Russian-Finnish Symp. on Radioastronomy, 1999*, p. 125.
11. http://www.sao.ru/hq/sun/obs_table.html.
12. http://www.sao.ru/hq/sun.
13. V. I. Garaimov, “Processing of one-dimensional vector data arrays in OS Windows. WorkScan program, version 2.3” [in Russian], preprint No. 127T, Special Astrophys. Obs. Russian Acad. Sci., Nizhny Arkhyz (1997).
14. S. Kh. Tokhchukova, “Implementation of the multi-azimuth regime of observations of the Sun at RATAN-600” [in Russian], preprint No. 174, Special Astrophys. Obs. Russian Acad. Sci., Nizhny Arkhyz (2002).
15. O. A. Golubchina, G. V. Zhekanis, V. M. Bogod, et al., in: *Solar Researches in the South-Eastern European Countries: Present and Perspectives, 24–28 April 2001, Bucharest, Romania*, Editura Academiei Romane (2002), p. 18.
16. M. I. Agafonov and O. A. Podvoiskaya, *Radiophys. Quantum Electron.*, **32**, No. 6, 559 (1989).
17. B. S. Minchenko, “Synthesis of two-dimensional images using the RATAN-600 radio telescope” [in Russian], Ph.D. Thesis Phys.-Math. Sci. (1979).
18. V. M. Bogod and S. Kh. Tokhchukova, *Astron. Lett.*, **29**, No. 4, 263 (2003).
19. R. A. Sych and Y.-H. Yan, *Chinese J. Astron. Astrophys.*, **2**, 183 (2002).
20. S. Tokhchukova and V. Bogod, *Solar Phys.*, **212**, No. 1, 99 (2003).